Fermilab FERMILAB-Conf-08-025-APC February 2008

Residual Activation of Accelerator Components*

I. L. Rakhno, N. V. Mokhov, S. I. Striganov
Fermilab, P.O. Box 500, Batavia, Illinois 60510

February 28, 2008

Abstract—*A method to calculate residual activation of accelerator components is presented. A model for residual dose estimation for thick objects made of arbitrary composite materials for arbitrary irradiation and cooling times is employed in this study. A scaling procedure is described to apply the model to thin objects with linear dimensions less than a fraction of a nuclear interaction length. The scaling has been performed for various materials and corresponding factors have been determined for objects of certain shapes (slab, solid and hollow cylinder) that can serve as models for beam pipes, magnets and collimators. Both contact residual dose and dose attenuation in the air outside irradiated objects are considered. A relation between continuous and impulse irradiation is accounted for as well.*

1 INTRODUCTION

Induced activation of accelerator components is an important issue from practical standpoint and correct prediction of residual activity is of primary importance when planning on various hands-on and maintenance procedures. While most of the values predicted with modern Monte Carlo codes for high energy accelerator environments can be obtained with a rather high accuracy, residual dose rates remain less reliable because of the complicated nature of this phenomenon and its sensitivity to the composition of irradiated materials. A multi-step approach based on a hadron transport code coupled to a nuclide transmutation inventory code (*e.g.*, CINDER [1] and DeTra [2]) or direct modeling [3] would provide the most reliable solution of activation problems. In practice a simplified approach is used: residual dose is determined using calculated distributions of star density and particle flux as well as precalculated star-to-dose and flux-to-dose conversion factors, respectively [4]. This approach is suitable for thick objects with linear dimensions exceeding some fraction of a nuclear interaction length. For thin objects this procedure gives rise to an overestimated residual dose. Direct measurements performed at CERN in the early 70s [5] revealed that measured residual dose for thin objects is lower than predicted one within a factor of three and the disagreement depends on material and size of the object.

In this paper the essentials of the method developed to determine the conversion factors for thick objects [6]-[8] are described and a scaling procedure for thin objects [9] is introduced. The scaling factors are calculated for objects of certain shapes that are important from practical standpoint. Distribution of residual dose in the air surrounding irradiated objects is considered. Beam pulse structure and repetition rate are taken into account as well.

2 MODEL FOR CONTACT RESIDUAL DOSE OF THICK OBJECTS

In the approach based on so-called ω-factors, one converts the density of inelastic nuclear interactions above 50 MeV (star density) to a contact residual dose rate for various combinations of irradiation (T_i) and cooling (T_c) times. The concept of ω-factors was introduced more than three decades ago [4]. It is based on the assumption that a high-energy inelastic interaction of a projectile hadron with a target nucleus (*star*) generates a number of radioactive nuclei so that for the average resulting radioactivation one can perform a simple parametrization that depends only on the target material. For a semi-infinite body the residual dose rate on its surface is described as follows:

$$\frac{dD}{dt} = \omega \frac{d^2S}{dVdt}\,, \qquad (1)$$

where $d^2S/dVdt$ is the star density production rate which is assumed to be uniform over the volume of the body. This model is a rather crude approach to reality [10]. It has been shown [11] that a 20 MeV star threshold should be used instead of the historical 50 MeV because of a non-zero contribution from spallation reactions in the 20–50

*Work supported by Fermi Research Alliance, LLC under contract No. DE-AC02-07CH11359 with the U. S. Department of Energy.

MeV region. In addition, residual activation reveals a dependence on projectile energy spectrum. The ω-factors describe the residual dose due only to emission of γ-quanta [8]. As long as we do not consider very thin objects the contribution from β-decays can be neglected.

An elaborate set of the ω-factors was described in [6, 7] where three major energy groups responsible for radionuclide production were defined: (1) above 20 MeV, (2) 1 to 20 MeV, and (3) below 0.5 eV. The energy groups were chosen to consider separately the most important nuclear reactions responsible for induced radioactivation in the regions: high energy inelastic interactions (mostly spallation reactions), threshold reactions $(n,2n)$, (n,p) *etc*, and (n,γ) reactions, respectively. Detailed calculations were performed for cascades induced by energetic hadrons in various samples [3]. Decay chains of created radionuclides were followed with the DeTra code in order to determine the emission rates of de-excitation photons for 12 hours$< T_i <$20 years and 1 sec$< T_c <$20 years. Corresponding dose rates on the outer surfaces were calculated from photon fluxes and related to the star density above 20 MeV and neutron fluxes in two other energy groups. A sophisticated interpolation algorithm, linked to the created database of material- and time-dependent ω-factors (see Fig. 1 (left) as an example), was developed and implemented into the MARS code [12].

3 SCALING PROCEDURE FOR THIN OBJECTS

For a thin object, *e.g.* a beam pipe, the geometry scaling factor, R_G, is defined as a ratio D_2/D_1, where D_2 and D_1 are dose rates calculated on the surface of the thin and a thick object, respectively, other things (material and specific activity) being equal. Isotropic, spatially uniform and monoenergetic 1-MeV gammas—as representatives of nuclear gamma decays due to spallation reactions—are used in these calculations to simulate a residual activity source term [9]. The MCNP code [13] is used in the calculations.

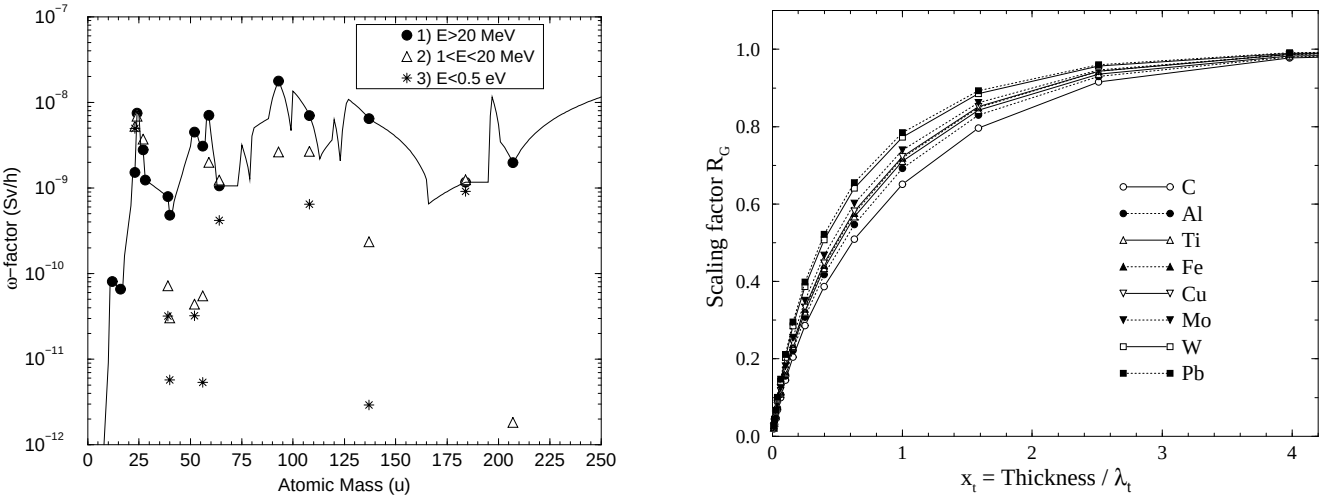

Figure 1: *Left*—An example of ω-factor dependence on mass of a target nucleus for three energy groups and T_i=30 days and T_c=1 day. Normalization is per $star/cm^3/s$ for $E > 20$ MeV, and per $neutron/cm^2/s$ for the other groups. The symbols represent results of a previous study [8] and the curve is an interpolation of the results of the study and those of an earlier one [10] for the high energy group. *Right*—The calculated scaling factors, R_G, for slabs of various materials. The lines are drawn to guide the eye.

3.1 Slab and solid cylinder

The calculated scaling factors for slabs are given in Fig. 1 (right). The data was fitted as follows:

$$R_G = \left(1 - \exp^{-Bx_t}\right)^C, \qquad (2)$$

where R_G is the scaling factor, $x_t = thickness/\lambda_t$ for slabs and $x_t = diameter/\lambda_t$ for cylinders, and a mean free path of 1-MeV γ-rays in the material, λ_t, is equal to $(N\sigma_t)^{-1}$, where N is atomic density and σ_t is total microscopic interaction cross section. Fitting parameters B and C are given in Fig. 2 (left). The advantage of using Eq. (2) is in the fact that it provides correct asymptotic values for the geometry scaling factor, R_G, at both $x_t \to 0$ and $x_t \to \infty$ independently of the values of the parameters B and C. The dependence shown in Fig. 2 can, in turn, be described by the following expressions:

$$B = B_{s0} + \sum_{n=1}^{4} B_{sn} A^n, \qquad (3)$$

$$C = C_{s0} + C_{s1} A, \qquad (4)$$

where A is atomic mass and the expansion coefficients B_{sn} and C_{sn} are given in Table 1. Other things being equal, for cylinders the increase in the scaling factor with diameter is slower than that for slabs because the cylinders can be considered to be infinite only in one dimension.

3.2 Hollow cylinder

For hollow cylinders one takes into account only beryllium, aluminum, and iron. It was found that the difference in the calculated scaling factors between beryllium and iron is about 15-20% so that an interpolation procedure for other materials is justified. The fitting was performed using the same Eq. (2), with x_t being $(R_{out} - R_{in})/\lambda_t$. The fitting parameters B and C are described as follows:

$$B = B_{h0} + B_{h1} \exp^{-x_t/x_0}, \quad (5)$$

$$C = C_{h0} + \sum_{n=1}^{3} C_{hn} x_t^n, \quad (6)$$

where B_{hn}, C_{hn}, and x_0 are given in Table 1.

4 ATTENUATION OF RESIDUAL DOSE IN THE AIR

The residual dose in the air due to residual activity of an irradiated object, $D(x,y,z)$, assuming isotropic angular distribution of the γ-rays emitted from the surface of the object, can be described as follows:

$$D(x,y,z) = k_d\ \phi(x,y,z) = k_d \int dS \frac{A_s}{2\pi\rho^2}, \quad (7)$$

where (x,y,z) are Cartesian coordinates of the observation point, $\phi(x,y,z)$ is flux of γ-rays, A_s is the surface emission rate of γ-rays per unit area and per solid angle of 2π, ρ is distance between the observation point and the surface element dS, k_d is a flux-to-dose conversion factor [13]. Energy dependence is omitted for simplicity's sake.

In the case of uniform spatial activation of an infinite cylindrical object one can make use of symmetry and the integral can be expressed in a closed form:

$$D(r) = \frac{D_0}{1 + r/R}\ F(\varphi\backslash\alpha), \quad (8)$$

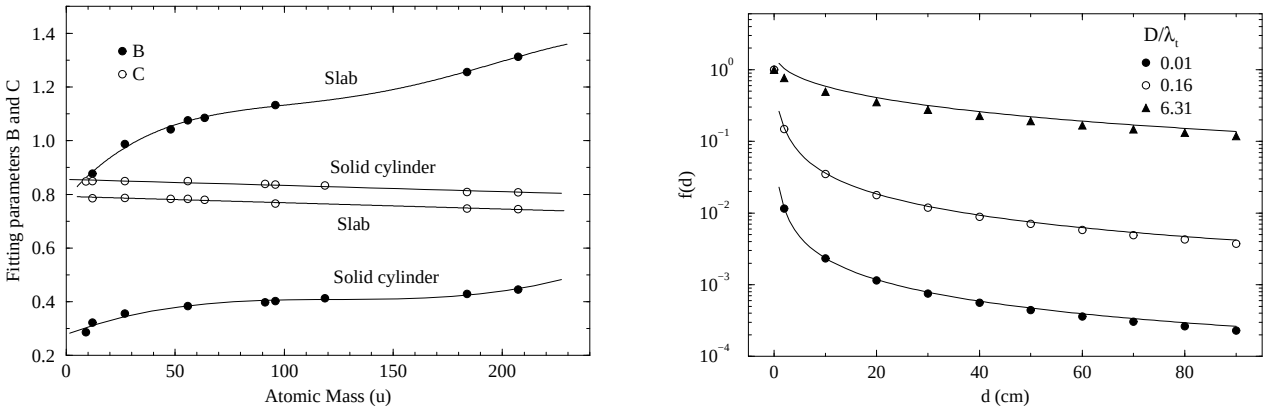

Figure 2: *Left*—Fitting parameters B and C from Eq. (2) *vs* atomic mass. The circles are results of calculations and the lines are results of fitting. *Right*—Dose attenuation function, $f(d)$, calculated according to Eqs. (8)-(10) (lines) and with the MCNP code (symbols) in the air around aluminum cylinders of diameter D *vs* the radial distance from the side surface of the cylinder, $d = r - R$.

Table 1: Expansion coefficients for slabs and solid cylinders (left) as well as for hollow cylinders (right)

	Slab	Solid cylinder
B_{s0}	7.8426×10^{-1}	2.7839×10^{-1}
B_{s1}	9.39×10^{-3}	3.06×10^{-3}
B_{s2}	-1.00765×10^{-4}	-2.42745×10^{-5}
B_{s3}	5.00304×10^{-7}	6.50166×10^{-8}
B_{s4}	-8.36463×10^{-10}	0
C_{s0}	7.9241×10^{-1}	8.5604×10^{-1}
C_{s1}	-2.35408×10^{-4}	-2.29036×10^{-4}

	Beryllium	Aluminum	Iron
B_{h0}	1.4428	1.9489	2.1151
B_{h1}	-0.85396	-1.21355	-1.3309
x_0	1.7464	2.1108	2.0774
C_{h0}	8.6847×10^{-1}	8.5445×10^{-1}	8.5947×10^{-1}
C_{h1}	1.4330×10^{-2}	3.2520×10^{-2}	3.0440×10^{-2}
C_{h2}	-3.010×10^{-3}	-5.930×10^{-3}	-5.590×10^{-3}
C_{h3}	1.3174×10^{-4}	3.0188×10^{-4}	2.8175×10^{-4}

$$\varphi = \arcsin\sqrt{\frac{1+R/r}{2}}, \quad \alpha = \arcsin\left(\frac{2\sqrt{r/R}}{1+r/R}\right), \qquad (9)$$

$$f(r-R) \equiv \frac{D(r)}{D_0}, \qquad (10)$$

where $F(\varphi\backslash\alpha)$ is an incomplete elliptic integral of the first kind [14], R is radius of the cylinder, D_0 is residual contact dose on the surface of the cylinder, $r = \sqrt{x^2+y^2+z^2}$ and f is the dose attenuation function.

Due to the ρ^{-2} dependence used in Eq. (7), there is a singularity when the observation point approaches surface of the cylinder, $r \rightarrow R$. In such a case $\alpha \rightarrow \pi/2$, $\varphi \rightarrow \pi/2$, and $F(\varphi\backslash\alpha) \rightarrow \infty$. From practical standpoint, one can eliminate the problem just by removing from consideration the points that are very close to the surface. A comparison between results of modeling with the MCNP code and Eqs. (8)-(10) is shown in Fig. 2 (right).

5 CONTINUOUS AND IMPULSE IRRADIATION

For a continuous irradiation in the case of a single radionuclide the induced activity, A_c, is expressed as follows:

$$A_c \propto N_b(1-e^{-\lambda t}), \qquad (11)$$

where t is irradiation time, λ is a decay constant, N_b is the incident beam intensity. If one considers an impulse irradiation and the total number of projectiles, $N_b t$, is equally distributed between n short equidistant pulses, the induced activity, A_p, immediately after the n_{th} pulse is described as follows:

$$A_p = A_c \frac{\lambda\Delta}{e^{\lambda\Delta}-1}\frac{e^{\lambda\Delta}-e^{-\lambda t}}{1-e^{-\lambda t}}, \qquad (12)$$

where $t = (n-1)\Delta$ and Δ is the time interval between the pulses. For long-lived nuclides $\lambda_L\Delta << 1$ and $A_p \simeq A_c$. For short-lived nuclides $\lambda_S\Delta >> 1$ and activity between pulses varies significantly. Immediately *after* the n_{th} pulse $A_p \simeq A_c\lambda_S\Delta$ and after that the activity drops rapidly. If a short-lived and long-lived radionuclides are generated in the impulse mode with cross sections σ_S and σ_L, respectively, their activities after cooling time, t_c, are expressed as $A_S \simeq A_L(\sigma_S/\sigma_L)\lambda_S\Delta e^{-\lambda_S t_c}$, so that for $t_c > \Delta$ one has $A_S << A_L$. In such a case the activity due to the impulse irradiation can be calculated using Eq. (11).

References

[1] W. B. WILSON, Los Alamos National Laboratory, LA-UR-93-3080 (1993).

[2] P.A. AARNIO, CERN, CMS Note-1998/086 (1998).

[3] http://www.fluka.org/.

[4] J. RANFT and K. GÖBEL, CERN, Internal Note HP-70-92 (1970).

[5] G. STEVENSON (private communication).

[6] I. RAKHNO, N. MOKHOV, A. ELWYN, N. GROSSMAN, M. HUHTINEN, L. NICOLAS, Fermi National Accelerator Laboratory, Fermilab-Conf-01/304-E (2001).

[7] M. HUHTINEN and L. NICOLAS, CERN, CMS Note-2002/019 (2002).

[8] M. HUHTINEN, "Radioactivation at Supercolliders,"*Proc. 42nd Workshop on Innovative Detectors for Supercolliders*, Erice, Sicily, Italy, 28 Sep. - 4 Oct., 2003, pp. 390-404, World Scientific, Singapore (2004).

[9] N. V. MOKHOV, E. I. RAKHNO, I. L. RAKHNO, Fermi National Accelerator Laboratory, Fermilab-FN-0788-AD (2006).

[10] M. HUHTINEN, CERN, TIS-RP/IR/98-28 (1998).

[11] M. HUHTINEN, CERN, CMS Note-1998/044 (1998).

[12] N. V. MOKHOV, Fermilab-FN-628 (1995); N. V. MOKHOV, K. K. GUDIMA, C. C. JAMES *et al.*, *Radiation Protection and Dosimetry*, **116**, p. 99 (2005); N. V. MOKHOV, S. I. STRIGANOV, "MARS15 Overview," *Proc. Hadronic Shower Simulation Workshop*, Batavia, Illinois, USA, 6-8 September, 2006, Vol. 896, pp. 50-60, American Institute of Physics, Melville, NY (2007); http://www-ap.fnal.gov/MARS/.

[13] "MCNP - A General Monte Carlo N-Particle Transport Code," LA-13709-M, J. F. BRIESMEISTER, Ed., Los Alamos National Laboratory (2000).

[14] *Handbook of Mathematical Functions*, pp. 589-618, M. ABRAMOWITZ and I. A. STEGUN, Eds., Dover Publications, Inc., New York, NY (1970).